

Green synthesis, spectral characterization, microbial activities, and antioxidant activities of cobalt oxide nanoparticles using *Aerva lanata* leaves extract

R.Manikandan^{1,2}, G.Vanitha¹, A.Prakasam^{1,3}, M.D.Navinkumar^{1,4}, K.Sathiyamoorthi⁵, B.Dhinakaran^{1*}

¹PG and Research Department of Physics, Government Arts College, Chidambaram, Tamilnadu, India– 608001.

²Munna College of Education, Parangipettai, Tamil nadu, India-608502

³PG& Research Department of Physics, Aringar Anna Arts College, Villupuram, Tamilnadu, India-605602

⁴Vivekanadan College of Education, Puducherry, India-605008

⁵PG and Research Department of Chemistry, Government Arts College, Chidambaram, Tamilnadu, India– 608001.

*Corresponding author

e-mail: drbdphysics@gmail.com

Abstract

In the present study, cobalt nanoparticles were synthesized by cost effective method using *Aerva lanata* leaves extract and characterized using various techniques such as UV-visible spectrophotometry, Fourier transform infrared spectrometry(FT-IR), Fluorescence spectroscopy(FL), and Scanning electron microscopy(SEM) coupled with Energy dispersive micro analysis(EDS) and XRD. The spectroscopic methods confirmed the formation of cobalt nanoparticles and the microscopic technique confirmed the shape and size of the cobalt nanoparticles as spherical. Antibacterial activity of the synthesized nanoparticles was measured by zone inhibition method. The cobalt nanoparticles showed effective antibacterial activity against human pathogenic bacteria such as *Pseudomonas Aeruginosa* and *Escherichia coli*. The usage of plant extract for the preparation of Cobalt nanoparticle makes the process cost effective, non-hazardous and green method.

Keywords: Green synthesis, *Aerva lanata*, Co_3O_4 NPs, Characterizations, Microbiological Activities and Antioxidant activity.

1. Introduction

Nanoparticle research is presently an area of strong scientific interest due to a wide variety of potential application in biomedical, optical and electronic fields. Cobalt is considered to be the first catalyst made from nonprecious metal with properties closely matching with those of platinum [1]. The shape and size of the nanoparticles influence the physical characterization of these novel materials. Nanoparticles are the nano-sized particles [2-3] which have found various applications in the fields of medicine [4-7], biology [8-11], catalysis [12-14] etc. The nanoparticles can be synthesized by physical, chemical or biological methods. Cobalt nanoparticles can be synthesized by various approaches like ultrasonic spray pyrolysis, DC magnetron sputtering [15], thermal decomposition [16], electrochemical [17] and Liquid-Phase Reduction [18] process and also by biological methods such as microbial synthesis [19] of nanoparticles. Recently, many studies have proven that the plant extracts act as a potential originator for the synthesis of the nanomaterials in harmless ways. The plants are used successfully in the synthesis of several greener nanoparticles such as cobalt, copper, silver, gold, palladium, platinum, zinc oxide and magnetite. Plant mediated biological synthesis of nanoparticles is gaining importance due to its simplicity, cost effective and eco-friendliness [20-21]. Cobalt nanoparticles could be efficient nanoparticles as they possess good catalytic [22-23] and high performance permanent magnetic properties [24-25] and also possess biomedical [26] and cytotoxic

[27] activity. Medicine for splenomegaly; this herb is used to dissolve kidney stones and reduce blood and whiteness in urine.

2. Material and Methods

2.1. Collection of Sample

Fresh *Aerva lanata*(sirukan peelai) leaves were collected from botanical garden, Department of Botany, Government arts college, Chidambaram. Leaves were washed in three times thoroughly by running ordinary tap water (OTW), then washed two times with double distilled water (DDW) to remove any dust particles on the leaves, washed leaves were allowed to dry in air at room temperature. The dried leaves were grained and powdered by using electric mixer. This powder was used to prepare the leaves extracts

2.2. Chemicals, Solvents and Starting Materials

De-ionized water, whatmann 1 μ and whatmann 41 μ filter papers, cobalt nitrate hexa hydrate ($\text{Co}(\text{NO}_3)_2 \cdot 6\text{H}_2\text{O}$), Sodium hydroxide pellets, hydrochloric acids, sulphuric acid, vitamin C, Acrobose, Diclofenac sodium, Muller Hinton agar(MHA), Sabouraud Dextrose agar(SDA), sodium phosphate, ammonium molybdate, Amylase, DNSA reagent, Dimethyl formamide, Bovine serum albumin solution, 3-[4,5-dimethylthiazol-2-yl]-2, 5-diphenyl tetrazolium bromide, tetrazolium, phenol red, DMSO, and other chemicals were purchased from Merck (India) Ltd. All chemicals were used without further purification.

2.3 Instruments and equipment

Electric oven, Magnetic stirrer (REMI 2 MLH), E-1 portable TDS & EC meter, pH-009(I)A pen type pH meter, petri plate, ordinary incubator, CO₂ incubator, Micro Plate reader, Inverted microscope, Refrigerated centrifuge, sterilized 250ml separating funnels, sterilized conical flasks, sterilized 400ml beakers, watch glasses, 7'' funnels, glass rods, and 10ml measuring cylinders,

2.4. Plant material processing

5 grams of *Aerva lanata* (Sirukan peelai) leaves powder with 50 mL of double-distilled water (DDW) taken in the 250 mL round bottomed flask, water condenser fitted and fix the running tap water then heated for 20 min at 80^o C. Then the extract was filtered with Whatman 1# filter paper. The filtrate was used to the further green synthesis of process

2.5. Biosynthesis procedure

For the synthesis of Cobalt oxide nanoparticles by reducing cobalt nitrate hexahydrate (M.F:Co(NO₃)₂.6H₂O, MW: 291.04 g/mol), 180 mL of homogenous solution of cobalt nitrate is steadily mixed with 10mL of *Aerva lanata* (Sirukan peelai) leaves extract followed by continuous heating (70 °C) and stirring at 500 rpm for 3 hr at magnetic stirrer with heating instrument, to achieve reddish pink solution [28], The obtained brownish red colour solution was added with 0.1M NaOH solution maintain by pH 10, the solution was changed to blue colour precipitate. The obtained precipitate was filtered by whatmann 1# filter paper. The precipitate was dried and powdered then calcinated at 350°C through muffle furnace. After calcination to obtained gray colour fine crystalline cobalt oxide nanoparticles. Finally, Co₃O₄NPs were steadily characterized. Figure.1, have shown in scheme of green synthesis of cobalt oxide nanoparticles.

2.6 Physicochemical Characterization

The absorption properties of the biosynthesized Co₃O₄NPs and the fruit extract was examined by UV-Visible spectroscopic technique (UV-1601 Shimadzu spectrophotometer) using DMSO at a resolution of 1 nm, in the wavelength range of 400–800 nm. FT-IR measurement was done using FTIR8400S-spectrophotometer (Shimadzu, International, Co. Ltd, Tokyo, Japan) to determine the different types of chemical bonds between bioactive compounds of extract and cobalt oxide solution. Samples were scanned from 400–4000 cm⁻¹ with potassium bromide pellets. The representative peaks of the cobalt oxide group with NP are expressed in a reciprocal wavelength (cm⁻¹).The wide-angle X-ray diffraction (XRD, Bruker AXS D8) spectra were measured on a powder diffractometer with nickel-filtered Cu Ka, X-ray beam (λ= 0.15418 nm).The morphology and

the particle size of the nanoparticles were investigated by Scanning

Electron microscope and Transmission Electron Microscope. The images were observed with the help of an electron microscope (VEGA3SB, TESCAN, and Czech). Energy Dispersive X-ray (EDS) spectroscopy (a part of SEM which was done using Quantax 200 with X FlashR 6130) was used for detecting the arrangement of elements in the sample. For the Transmission Electron Microscope (TEM) (Model: JEM-2010, JEOL, Japan) analysis, diluted and dispersed solutions of cobalt oxide nanoparticles were dropped onto a copper grid (~200 mesh), dried and observed at 200KV.

2.6 Microbiological activities

Antibacterial of extracts was determined by disc diffusion method on Muller Hinton agar (MHA) medium. Muller Hinton Agar (MHA) medium is poured in to the petriplate. After the medium was solidified, the inoculums were spread on the solid plates with sterile swab moistened with the bacterial suspension. The disc were placed in MHA plates and add 20 µl of sample (Concentration: 1000µg, 750µg and 500 µg) were placed in the disc .The plates were incubated at 37°C for 24 hrs. Then the antimicrobial activity was determined by measuring the diameter of zone of inhibition. The antimicrobial activities of cobalt oxide nanoparticles were tested against bacterial species like three gram-negative (*Staphylococcus aureus*, *Proteus vulgaris*, *Salmonella typhimurium*) & two gram-positive (*Escherichia coli*, *Bacillus subtilis*)

Antifungal activity of the Sample was determined by disc diffusion method on Sabouraud Dextrose agar (SDA) medium. Sabouraud Dextrose agar (SDA) medium is poured in to the petriplate. After the medium was solidified, the inoculums were spread on the solid plates with sterile swab moistened with the fungal suspension. Amphotericin-B is taken as positive control. Samples and positive control of 20 µl each were added in sterile discs and placed in SDA plates. The plates were incubated at 28°C for 24 hrs. Then antifungal activity was determined by measuring the diameter of zone of inhibition. Anti-fungal activity of cobalt oxide nanoparticles against fungal strains like *Candida albicans*, *Trichoderma viride*. Well diffusion method at room temperature. The zones of inhibition were measure and recorded.

2.7 Anti-oxidant activity

DPPH ASSAY:

DPPH (1,1-diphenyl-2-picrylhydrazyl) is characterised as a stable free radical by virtue of the delocalisation of the spare electron over the molecule as a whole, so that the molecules do not dimerise, as would be

the case with most other free radicals. The delocalisation also gives rise to the deep violet colour, characterized by an absorption band in ethanol solution centered at about 520 nm. When a solution of DPPH is mixed with that of a substance that can donate a hydrogen atom, then this gives rise to the reduced form (Blois,1958) with the loss of this violet colour (although there would be expected to be a residual pale yellow colour from the picryl group still present). Representing the DPPH radical by Z• and the donor molecule by AH, the primary reaction is

$Z\bullet + AH = ZH + A\bullet$
where ZH is the reduced form and A• is free radical produced in this first step. This latter radical will then undergo further reactions which control the overall

3. Result and discussion

3.1 UV Spectral analysis

Figure 1 shows the UV-vis spectra of Cobalt oxide colloid obtained. The surface Plasmon resonance (SPR) band is broad indicating poly-dispersed

stoichiometry, that is, the number of molecules of DPPH reduced (decolorised) by one molecule of the reductant.

Aliquot 3.7 ml of absolute methanol in all test tubes and 3.8ml of absolute methanol was added to blank. Add 100µl of BHT to tube marked as standard and 100µl of respective samples to all other tubes marked as tests. 200µl of DPPH reagent was added to all the test tubes including blank. Incubate all test tubes at room temperature in dark condition for 30 minutes. The absorbance of all samples was read at 517nm.

$$\% \text{ Antioxidant activity} = \frac{(\text{Absorbance at blank}) - (\text{Absorbance at test})}{(\text{Absorbance at blank})} \times 100$$

nanoparticles. A smooth and narrow absorption band at 391.30 nm is observed which is characteristic of mono-dispersed spherical nanoparticles. UV-visible spectroscopy is one of the most widely used techniques for structural characterization of Cobalt oxide nanoparticles.

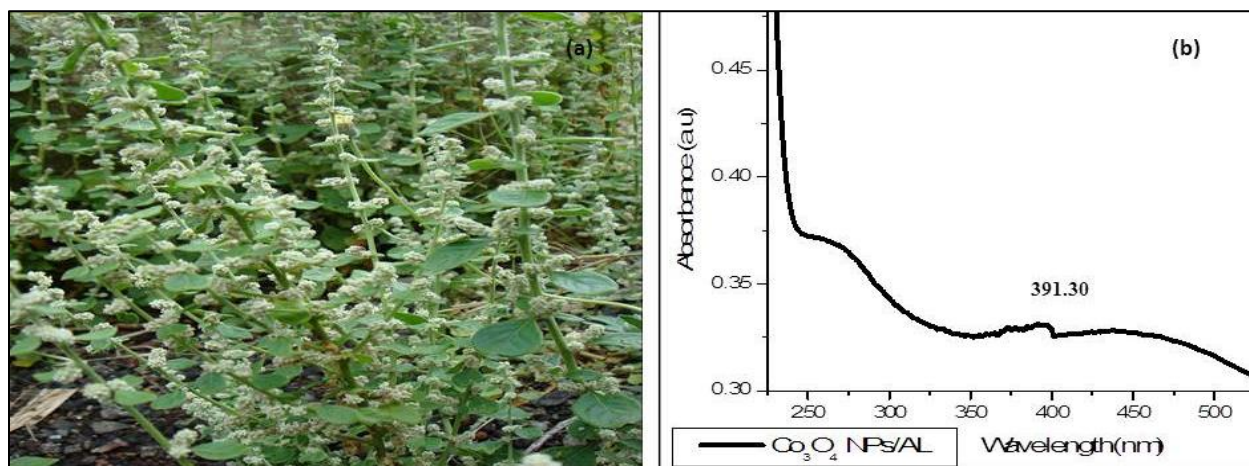


Figure 1. (a) Image of Aerva lanata (Sirukan peelai), (b) UV spectrum of Co₃O₄NPs by Aerva lanata (Sirukan peelai)

UV-Vis spectroscopy result showed that the typical peaks of Co₃O₄ NPs was detected in the range of maximum wavelength between 250-300 nm and 380-450 nm as shown in Fig. 1b. These peak indicated the transfer processes of Co (II) and Co (III) with oxygen, respectively. The surface plasmon resonance (SPR) band (λ max) around 391.30 nm broadened and slightly moved to the long wavelength region, indicating the presence and formation of Cobalt oxide nanoparticles [29]. The optical

absorption spectra of metal nanoparticles are dominated by surface Plasmon resonances (SPR), which shift to longer wavelengths with increasing particle size. The position and shape of plasmon absorption of cobalt oxide nanoclusters are strongly dependent on the particle size, dielectric medium, and surface-adsorbed species. The surface plasmon absorption of cobalt nanoparticles have the short wavelength band in the visible region around 391.30 nm is due to the transverse electronic oscillation.

3.2 FTIR Spectroscopy

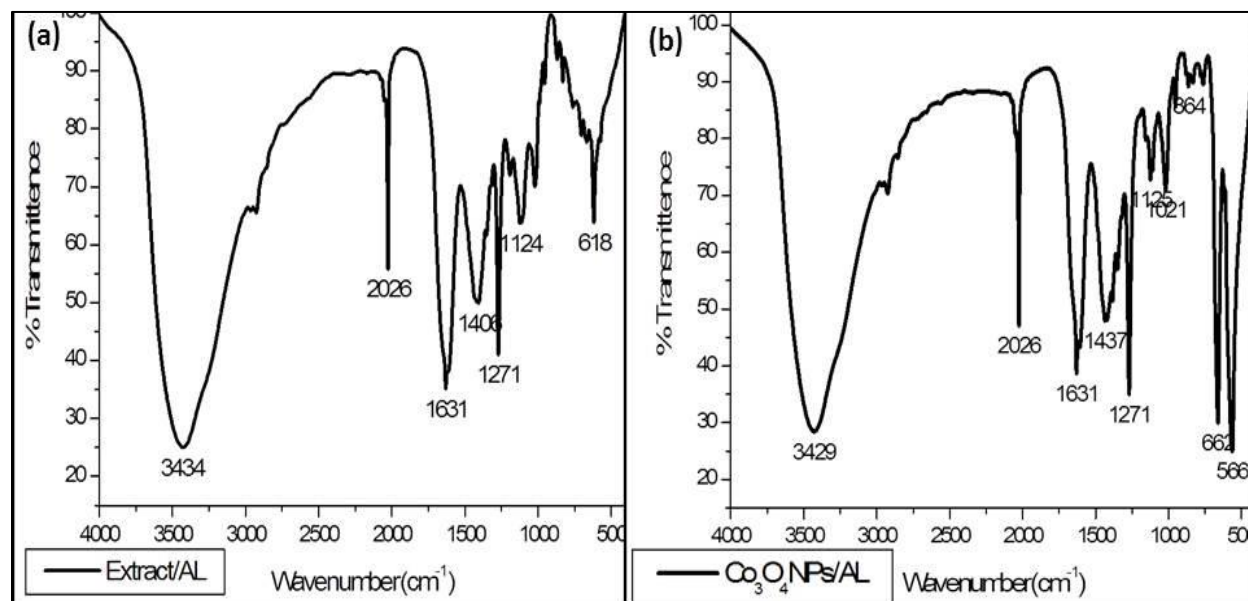


Figure 2. (a) FTIR Spectrum of Aerva lanata (Sirukan peelai) leaves extract, (b) FTIR spectrum of Co_3O_4 NPs by Aerva lanata (Sirukan peelai)

FTIR measurement was carried out to identify the possible biomolecules responsible for capping and efficient stabilization of Co nanoparticles synthesized using Aerva lanata (Sirukan peelai)

leaves aqueous extract. Figure-2(a) shows the FTIR spectrum of Aerva lanata (Sirukan peelai)

leaves aqueous extract and Figure-2(b) shows the FTIR spectrum of cobalt nanoparticles by Aerva lanata (Sirukan peelai) leaves aqueous extract. In the FTIR spectrum of aqueous extract of Ocimum Basilicum-Lamiaceae (Thiru Neetru Pathilai) leaves have shown in Fig:2(a) the sharp peak of 3434cm^{-1} have indicates $-\text{OH}$ stretching vibration, the sharp peak at 2026cm^{-1} have reveals that carbonyl bending vibrations, The sharp doublet peaks at 1631cm^{-1} have reveals that the carbonyl stretching vibrations, the peaks of 1406cm^{-1} have shown CH_2 & CH_3 deformation bending vibrations, The peaks of 1271cm^{-1} stretching vibration of $-\text{CN}$ bonding, the sharp peaks at 1271cm^{-1} have shown in O-H bending vibrations, the sharp peaks of 1124cm^{-1} have shown C-C-C bending vibration. The FTIR spectrum of cobalt nanoparticles by Aerva lanata (Sirukan peelai) leaves

aqueous extract have shown in Figure 2(b)., 3429cm^{-1} with decreased transmittance because cobalt metal ions reduce the various $-\text{OH}$ group containing group to alcohols, $-\text{C}-\text{H}$ stretching vibration of alkyl deformation also reduced by cobalt ions[30], The peaks of 1631cm^{-1} have shown reduced intensity having peaks compared with leave extract, this is the results for many organic functional groups are reduced and converted to CO to other alcoholic functional groups, The decreased peaks of 1437cm^{-1} have indicates $-\text{CH}_2-$ and $-\text{CH}_3$ bending vibrations, the peaks of 1126cm^{-1} have shown C-C-C bending vibration, The weak peaks at 1125 and 1047cm^{-1} were indicates The IR spectrum of cobalt oxide exhibits two major bands at 568cm^{-1} and $\sim 664\text{cm}^{-1}$. The first band is associated with the Co^{3+} vibration in the octahedral hole and the second band (ν) is attributed to the Co^{2+} vibration in the tetrahedral hole, which confirms the formation of the Co_3O_4 spinel. The above FTIR spectrum of leaves extract spectrum have shown only the water soluble phyto constituents, finally cobalt nanoparticles FTIR shown the reduced peaks cobalt ions³⁺ and cobalt ²⁺ ions reduced the various phytoconstituents.

3.3 Fluorescence spectroscopy

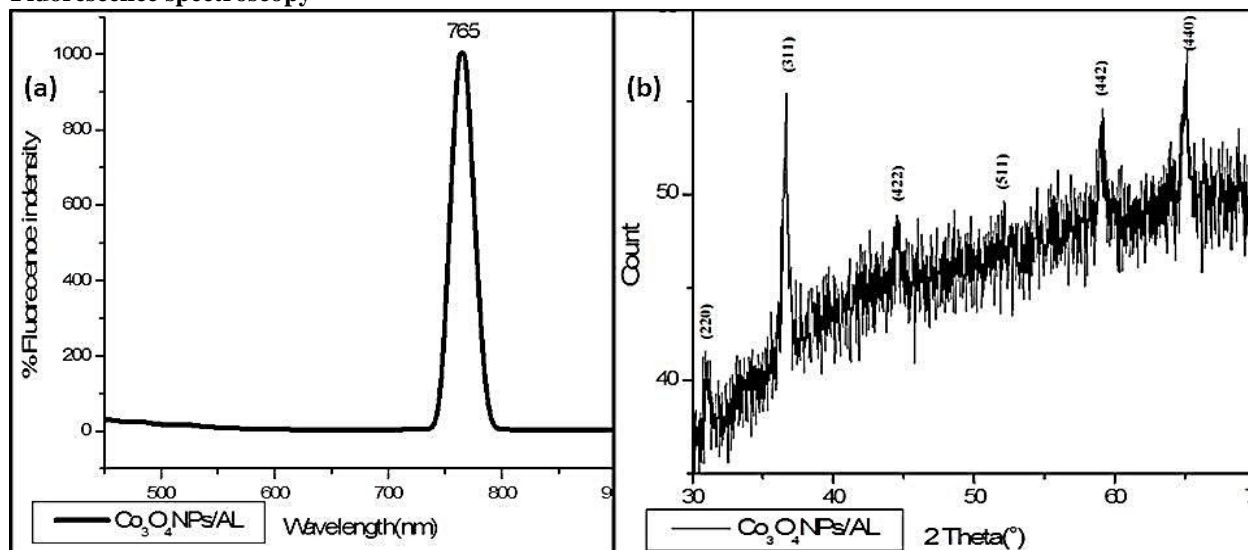


Figure 3. (a) FL Spectrum of $\text{Co}_3\text{O}_4\text{NPs}$ by *Aerva lanata* (Sirukan peelai), (b) XRD pattern of $\text{Co}_3\text{O}_4\text{NPs}$ by *Aerva lanata* (Sirukan peelai)

The spectral characteristics of fluorophores must match the wavelengths of the excitation light, Dichroic and emission filters of the fluorescence microscope on which the experiments are to be done. Moreover, it is advised that their spectra are well separated from the spectra of other fluorophores that will be used simultaneously in the experiments to minimize cross-talk and bleed through, which can give rise to false colocalization and misinterpretations if not appropriately corrected. For use with advanced optical techniques (such as higher solution microscopies, two-photon microscopy, fluorescence lifetime imaging, spectral imaging or correlation spectroscopy), further photo-physical aspects (e.g., lifetime, blinking, and environmental sensitivity) must also be taken into account. **Figure:3(a)** shows the fluorescence emission of cobalt nanoparticles ($\text{Co}_3\text{O}_4\text{NPs}$). It shows that the plasmonic resonance in the range close to 765 nm.

3.4 XRD Analysis

The crystalline nature of the cobalt oxide nanoparticles was evaluated by X-ray diffraction analysis.

In Figure 4, the XRD pattern of Co_3O_4 nanoparticles by *Aerva lanata* (Sirukan peelai) exhibits diffraction peaks with 2θ values of 30.84° , 37.99° , 44.16° , 54.89° , 58.53° , and 66.33° that are allocated to 220, 311, 422, 511, 442 and 440 crystal planes of the crystalline Co_3O_4 phase correspondingly. These peaks are indexed to a pure cubic phase structure (JCPDS Card No. 80–1540). The average crystalline size of the nanoparticles was calculated using the Scherer equation concerning the peaks (31). The average size of the synthesized Co_3O_4 nanoparticles was 36.24 nm.

3.5 SEM Analysis

The surface morphology of the nanoparticles was determined by analysing the structure by the scanning electron microscopy. SEM images in **Fig. 4(a-d)** showed irregular, cubic, hexagonal and spherical shapes of various sizes that are agglomerated [32-34]. Further observations with higher magnifications reveal that these images possess smooth surfaces. Surface morphology of Co_3O_4 NPs.

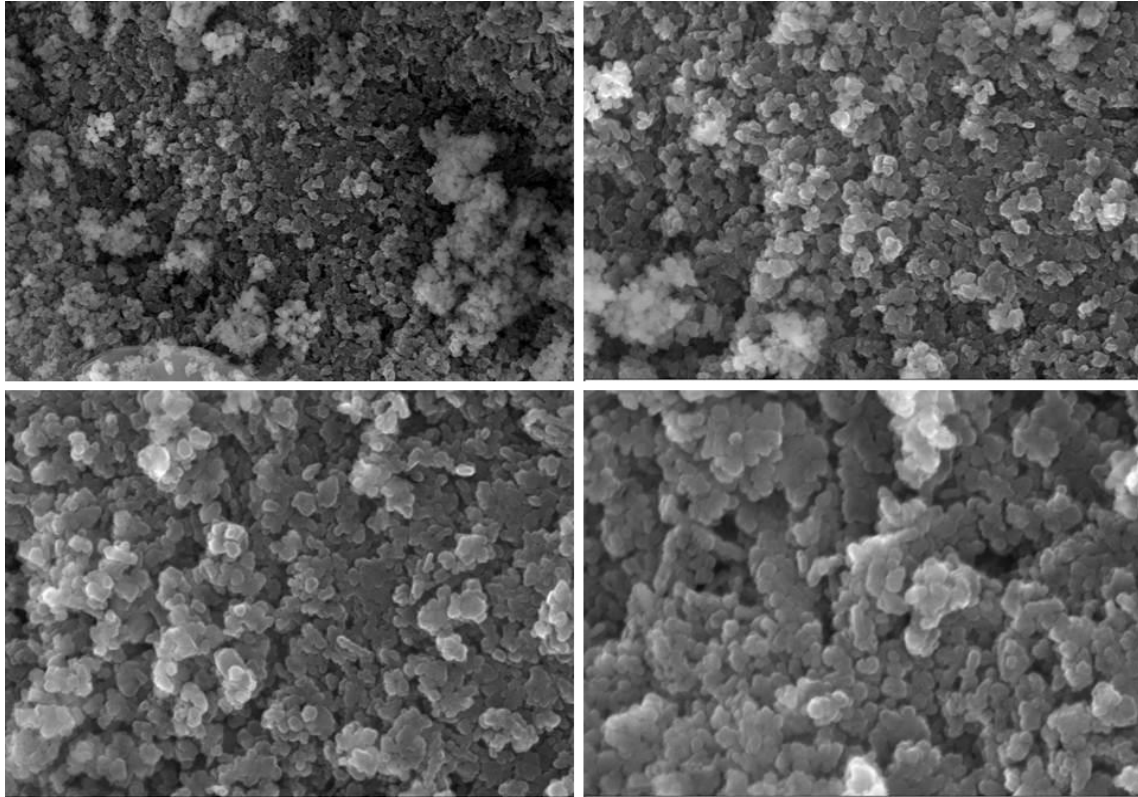


Figure 4. (a-d) FL SEM image of Co_3O_4 NPs by *Aerva lanata* (Sirukan peelai)

Biomolecules from leaf extract of *Aerva lanata* (sirukan peelai) acts as capping and stabilizing agent which form coating on the individual nanoparticles and contains hydroxyl group which causes intermolecular hydrogen bonding resulting in agglomeration. This agglomeration depends upon the nature and compounds present in the extract eco toxic properties of transition metal oxide are due to shape, small size, high chemical reactivity, biological activity and agglomeration tendency which cause threat to the environment and human beings.

3.6 EDS Analysis

The structural characterization of Co_3O_4 NPs was implemented utilizing an analysis of dispersive energy X-ray spectroscopy (EDX) as indicated in between 0 to 10 keV. **Figure:5a and 5b** shows the element quantitative and qualitative analysis may involve the formation of

Co_3O_4 NPs. The obtained results shows strong signals at 0.2 KeV, 0.6KeV, 0.8 keV, 6.8 keV and were for Co and intense signal between 0.0-0.5 keV for O suggesting that Co and O were the major elements and formation of synthesis of cobalt oxide arise from the sample and other unexpected weak signals at 0.3 keV, 1.9 keV, 2.1 keV, 2.7 keV, 3.1 keV and 9.8 keV were from bio-compounds present in the leaf extract. The analysis of the EDX spectrum also shown in the composition atom percentage of oxygen is $49.86 \pm 0.26\%$, mass percentage of oxygen is 21.26 ± 0.11 and atom percentage of cobalt is $50.14 \pm 0.22\%$. Mass percentage of cobalt is 78.74 ± 0.35 , other impurities are slightly presented. The trace amounts existence of cobalt demonstrated that plant phytochemical groups are involved in reducing and capping of synthesized Cobalt nanoparticles.

3.7 TEM Analysis

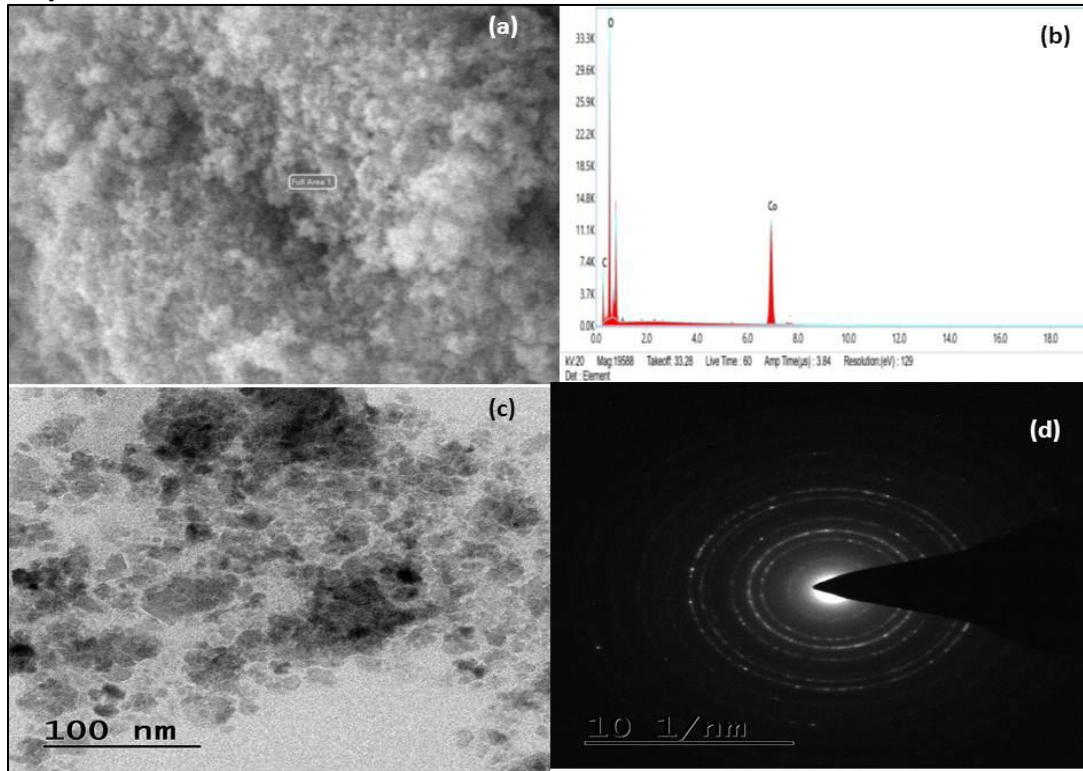


Figure 5. (a) EDS Micrograph image, (b) EDS Spectrum, (c) TEM Image (d) SAED pattern of $\text{Co}_3\text{O}_4\text{NPs}$ by *Aerva lanata* (Sirukan peelai)

The TEM micrographs of the biosynthesized $\text{Co}_3\text{O}_4\text{NPs}$ by *Aerva lanata* (Sirukan peelai) magnifications are shown in Fig. 5 (c). It was found that $\text{Co}_3\text{O}_4\text{NPs}$ were, spherical, hexagon, and triangular in shape with maximum particles in the size range of 100 nm. The SAED model confirmed the elemental $\text{Co}_3\text{O}_4\text{NPs}$ presence and also in agreement with the XRD analysis. The standard crystallite size of the $\text{Co}_3\text{O}_4\text{NPs}$ was estimated at 10.1 nm (Fig. 5(d)). The TEM picture demonstrated the cross-section borders between the two adjoining planes to be 5 nm separated which compares to the interplanar detachment of the [111] plane of face-focused cubic cobalt oxide.

3.8 Anti-microbial activity

3.8.1 Antibacterial activity

Antibacterial activities of synthesized $\text{Co}_3\text{O}_4\text{-NPs}$ by *Aerva lanata* (Sirukan peelai) have shown in Figure:6 (petri plates), Figure 8 have shown in cluster column chart of antibacterial activity of $\text{Co}_3\text{O}_4\text{-NPs}$ by *Aerva lanata* (Sirukan peelai). The antibacterial activities[35-37] were studied amongst both (Gram

positive and Gram negative) pathogenic bacteria. $\text{Co}_3\text{O}_4\text{NPs}$ showed maximum zone of inhibition against *Staphylococcus aureus* (9 mm) at 1000 mg/ml and 750 mg/ml concentrations this is good antibacterial activity of $\text{Co}_3\text{O}_4\text{-NPs}$ mediated by *Aerva lanata* (Sirukan peelai), $\text{Co}_3\text{O}_4\text{NPs}$ have shown moderate antibacterial activity against *Escherichia coli* (8 mm at 1000 mg/ml and 750 mg/ml), the worthy antibacterial activity have shown in $\text{Co}_3\text{O}_4\text{-NPs}$ against *Pseudomonas aeruginosa* bacterial strain the results also have shown concentration increases but activity of zone of inhibition does not change in three different concentration (10 mm at 1000mg/ml, 9mm at 750 mg/ml and 7 mm at 500 mg/ml) of the test solutions. Antibacterial activity of $\text{Co}_3\text{O}_4\text{NPs}$ against *Bacillus cereus* have shown unchanged activity (9 mm at 1000 and 750 mg/ml), 8mm at 500 mg/ml of the test solutions, for *Pseudomonas* bacterial strains in three different concentrations of test solutions (1000mg/ml, 750 mg/ml and 500 mg/ml), this is shown in moderate activity compared with standard antibacterial drug. The zone of inhibition values have shown in Table:1.

Table:1 Zone of inhibition of antibacterial activity of $\text{Co}_3\text{O}_4\text{-NPs}$ by *Aerva lanata*

(Sirukan peelai)

| Organisms | Zone of Inhibition (mm) | | | |
|------------------------|-----------------------------|-----|-----|----------|
| | Sample ($\mu\text{g/ml}$) | | | Standard |
| | 1000 | 750 | 500 | |
| Staphylococcus aureus | 9 | 9 | 8 | 11 |
| Escherichia coli | 8 | 8 | 7 | 12 |
| Pseudomonas aeruginosa | 10 | 9 | 7 | 11 |
| Bacillus cereus | 9 | 9 | 8 | 11 |

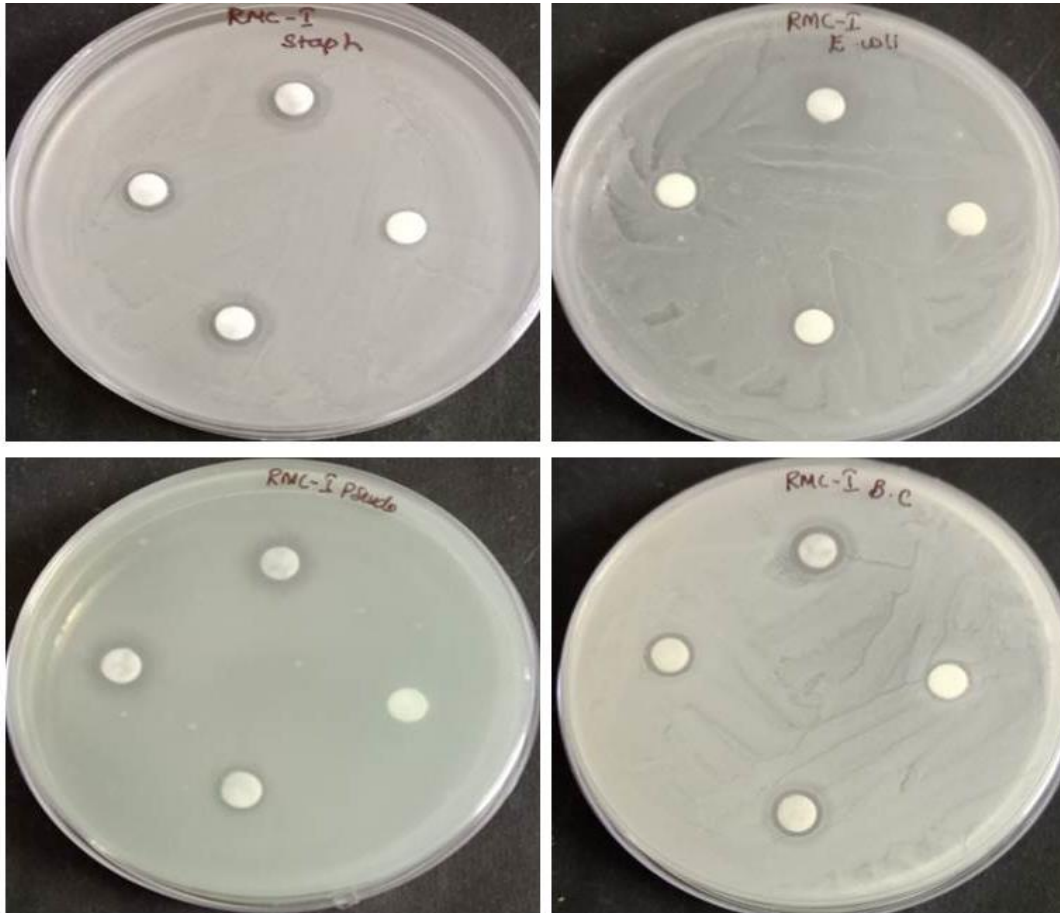


Figure 6. Petri plates of Antibacterial activity of Co_3O_4 -NPs by *Aerva lanata* (Sirukan peelai)

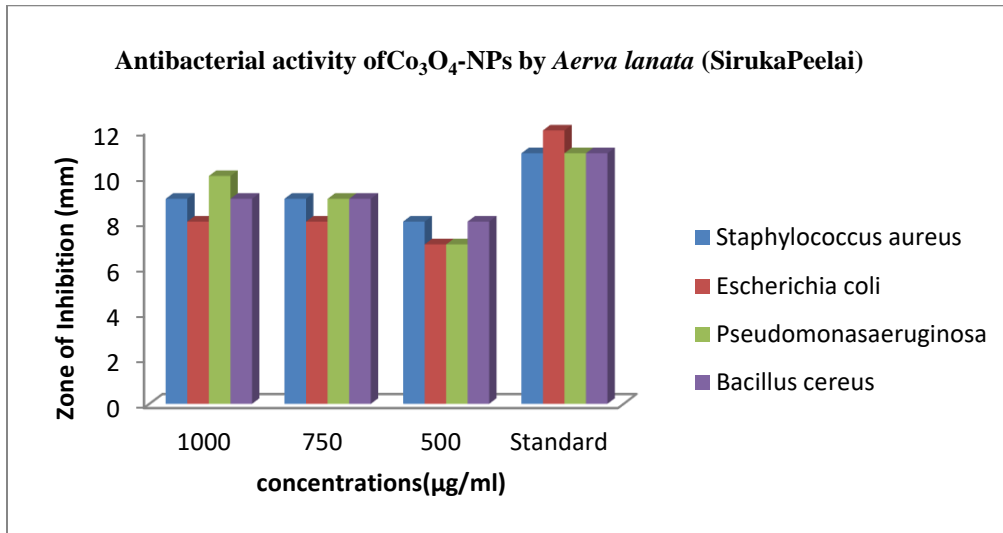


Figure 7. Cluster column of Antibacterial activity of Co_3O_4 -NPs by *Aerva lanata* (Sirukan peelai)

3.8.2 Antifungal activity

The antifungal activities of Co_3O_4 -NPs by *Aerva lanata* (Sirukan peelai) have shown moderate antifungal activity (Figure:8) against both the *Candida albicans* and

Trichoderma viride fungal strains in all the three concentrations solutions comparing Amphotericin-B (20 μl /disc) as standard antifungal medicine. The zone of inhibition values have shown in Table.2

Table:2 Zone of inhibition of antifungal activity of Co_3O_4 -NPs by *Aerva lanata* (Sirukan peelai)

| Organisms | Zone of Inhibition (mm) | | | |
|---------------------------|-----------------------------|-----|-----|----------|
| | Sample ($\mu\text{g/ml}$) | | | Standard |
| | 1000 | 750 | 500 | |
| <i>Candida albicans</i> | 9 | 8 | 7 | 21 |
| <i>Trichoderma viride</i> | 14 | 9 | 8 | 23 |

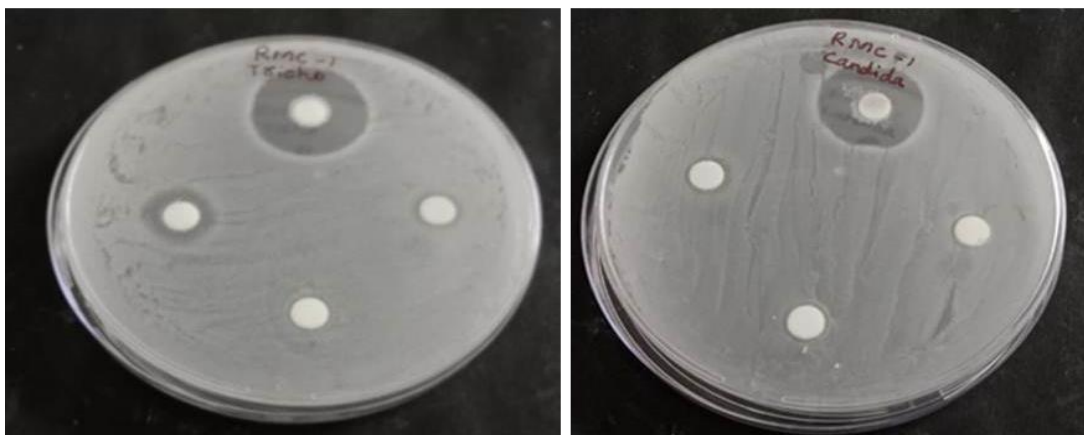


Figure 8. Petri plates of Antifungal activity of Co_3O_4 -NPs by *Aerva lanata* (Sirukan peelai)

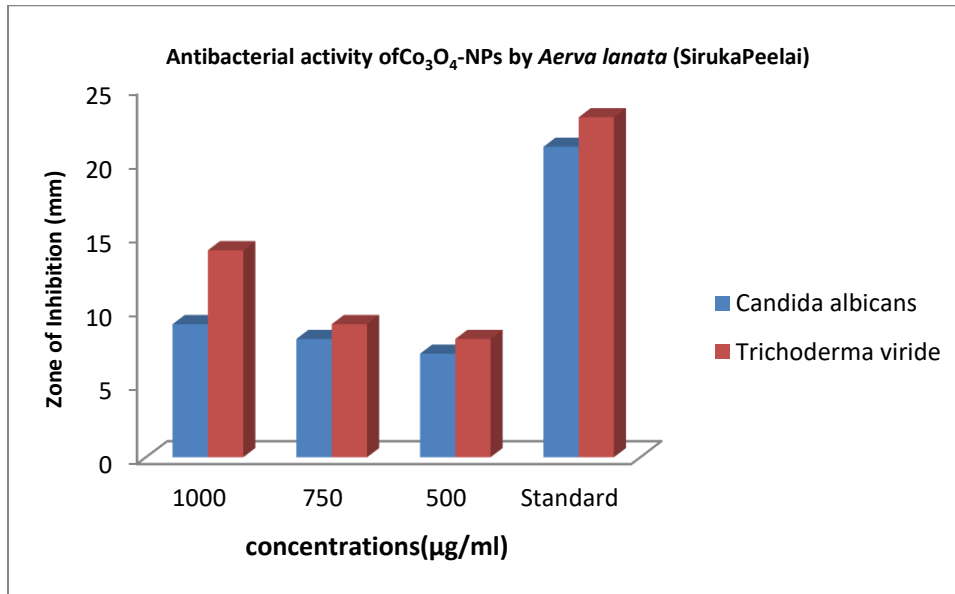


Figure 9. Cluster column of Antifungal activity of Co_3O_4 -NPs by *Aerva lanata* (Sirukan peelai)

3.9 Anti-oxidant activity

The DPPH assay is widely used for screening antioxidant activity because it is sensitive enough to detect active compounds at low concentrations [38]. DPPH is a nitrogen-centered free radical, and hence any compound that scavenges significant amounts of DPPH could reduce levels of other reactive nitrogen species in living cells. From our results, the biologically synthesized Co_3O_4 -NPs by *Aerva lanata* (Sirukan peelai) leaves extract quenched DPPH free radicals appreciably and dose-dependently (0 $\mu\text{g/ml}$, 40 $\mu\text{g/ml}$, 60 $\mu\text{g/ml}$, 80 $\mu\text{g/ml}$ and 100 $\mu\text{g/ml}$) (Figure.10). However, this activity was much lower than

that of the BHA standard. BHA is a pure antioxidant standard whose mechanism of action is accurately known[39-40]. Co_3O_4 -NPs by *Aerva lanata* (Sirukan peelai) however have no known mechanism of action as an antioxidant as this is one of the earliest reports on its antioxidant effect on DPPH free radicals. Hence, reason for its relatively lower antioxidant activity compared to DPPH cannot be adequately explained. It is therefore expedient to conducted further research into the mechanism of action of Co_3O_4 -NPs by *Aerva lanata* (Sirukan peelai) in scavenging DPPH free radicals.

Table:3 Antioxidant activity of Co_3O_4 -NPs by *Aerva lanata* (Sirukan peelai)

| S.NO | Concentration ($\mu\text{g/ml}$) | O.D VALUE | | | AVERAGE | DPPH % |
|------|------------------------------------|-----------|-------|-------|---------|--------|
| | | | | | | |
| 1 | 200 | 0.505 | 0.507 | 0.511 | 0.507 | 15.07 |
| 2 | 400 | 0.442 | 0.447 | 0.451 | 0.446 | 25.29 |
| 3 | 600 | 0.379 | 0.373 | 0.374 | 0.375 | 37.18 |
| 4 | 800 | 0.316 | 0.318 | 0.321 | 0.318 | 46.73 |
| 5 | 1000 | 0.241 | 0.236 | 0.233 | 0.236 | 60.46 |

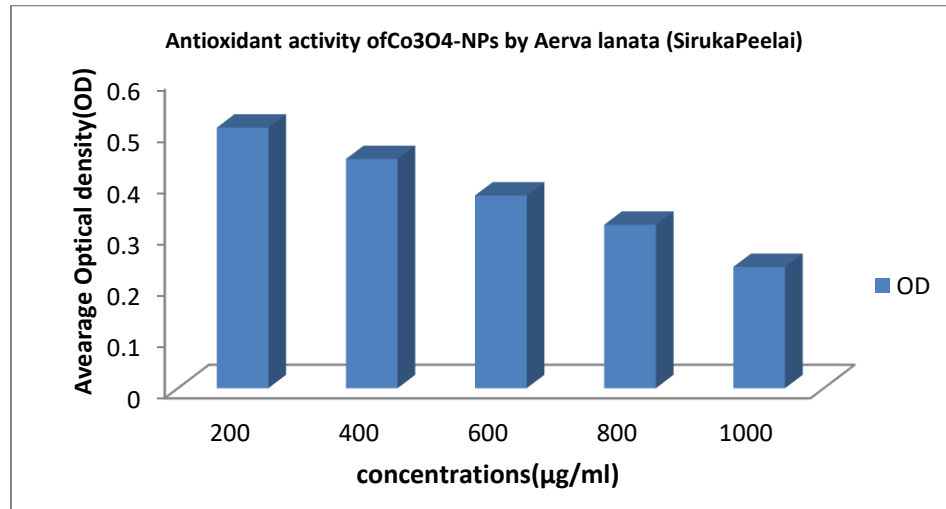


Figure 10. Cluster column of Antioxidant activity of Co₃O₄-NPs by Aerva lanata (Sirukan peelai)

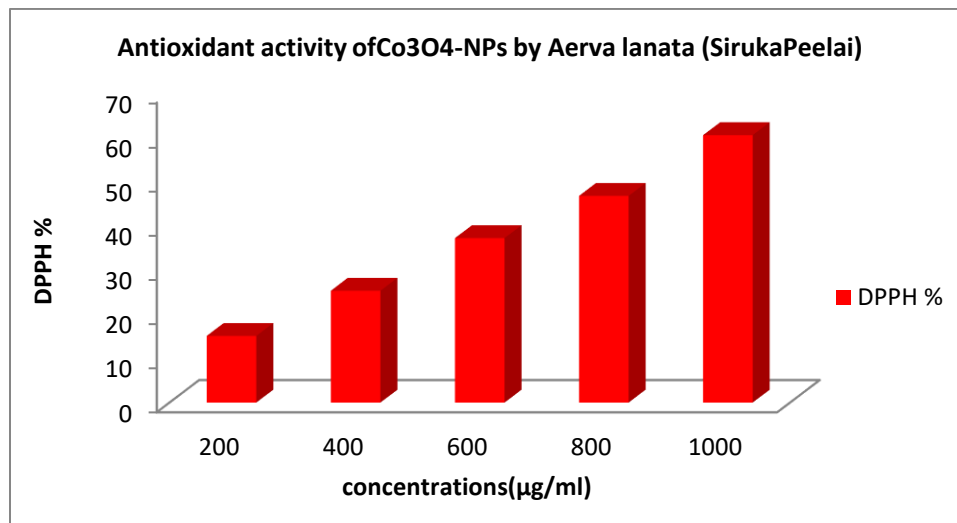


Figure 11. Cluster column of Antioxidant activity of Co₃O₄-NPs by Aerva lanata (Sirukan peelai)

Conclusion

Synthesis of Co₃O₄-NPs from the biological agent is eco-friendly, low-cost and proficient to synthesis at room temperature. The current research is developed an easy and eco-friendly method of synthesis of cobalt oxide nanoparticles using aqueous whole plant extract of Aerva lanata (Sirukan peelai). We have characterized the synthesized Co₃O₄-NPs using UV-vis spectroscopy, FTIR, FL, XRD, SEM, EDS and TEM analysis. The spectra of UV-vis confirmed the biosynthesized Co₃O₄-NPs supporting on surface plasmon resonance reading. XRD spectra confirmed the structure of FCC and crystalline nature in Co₃O₄-NPs. The reducing and capping of Co₃O₄-NPs are due to the presence of phytochemicals, which was confirmed by FT-IR spectra analysis. The SEM monograph revealed rod-shaped,

spherical, and triangular-shaped Co₃O₄-NPs. TEM micrograph displayed different shapes of synthesized Co₃O₄-NPs like spherical, pentagon, hexagon and triangular in shape with size between 50-100 nm. The synthesized Co₃O₄-NPs demonstrated maximum antibacterial activity against Gram negative bacterial pathogens (*Pseudomonas aeruginosa*) compared to Gram positive bacteria pathogen (*Staphylococcus aureus* and *Escherichia coli*). The synthesized Co₃O₄-NPs demonstrated favorable antioxidant activity against DPPH radicals and also shown high antioxidant activity. Thus, this safe and eco-friendly synthesis process can be used for the development of Co₃O₄-NPs which also demonstrate effective biological properties in the future. Further studies are necessary in order to get more applications of these biosynthesized Co₃O₄-NPs.

Reference

1. Y. Yu, A. Mendoza-Garcia, B. Ning, and S. Sun, *Advanced Materials*, 25, 22(2013).
2. L. J. Jongh. *Physics and Chemistry of Metal Clusters Compounds*, Kluwer Academic Publishers, Dordrecht (1994).doi:10.1007/978-94-015-1294-7.
3. G. B. Budkevich, I. B. Slinyakova and I. E. Neimark. *Colloid Journal*, 28,1(1996).
4. J.Kreuter, S. Gelperina. *S.Tumori*, 94, (2008).
5. K.Y. Yoon, B.J.Hoon, J.H. Park, J. Hwang, *Sci. Total Environ.*373(2007).
6. W. B. Tan, S.Jiang, Y.Zhang , *Biomaterials*, 28: pp.1565–1571, 2007.
7. Su J, Zhang J, Liu L, Huang Y, R.P.Mason, *Journal of Nanosci. Nanotechnol*, 8: pp.1174–1177, 2008.
8. L.R. Hirsch , R.J. Stafford , J.A. Barkson , S.R.Sershen ,B.Rivera , R.E.Price, J.D.Hazle,N.J. Halas,West JL. *PNAS*, 100: pp.13549-13554, 2003 .
9. Y.Matsumura, K.Yoshikata, S.Kunisaki, T.Tsuchido. *Appl. Environ. Microbio.* 69: pp.4278-4281,2003.
10. A.Ingle, A.Gade, S.Pierrat, C.Sönnichsen, M.Rai, *CurrNanosci*, 4:pp.141-4, 2008.
11. S.Pal, Y.K. Tak, J.M.Song. *Appl EnvironMicrobiol*, 73:1712-20,2007.
12. A.Nadiia, Ivashchenko, WojciechGac, A.Valenty, Tertykh, V.Viktor, Yanishpolskii, A.Sergei, Khainakov, V. Alla, Dikhtiarenko, Sylwia Pasieczna-Patkowska, Witold Zawadzki. *World Journal of Nano Science and Engineering*, 2: pp.117-125,2012. 28.
13. M.Muneer, Ba-Abbad, Abdul Amir H. Kadhum, Abu Bakar Mohamad, S.Mohd, Takriff, Kamaruzzaman Sopian. *Synthesis and Catalytic Activity of TiO₂ Nanoparticles for Photochemical Oxidation of Concentrated Chlorophenols under Direct Solar Radiation*, 7: pp.4871-4888,2012.
14. Chao Lin, Kai Tao, DayinHua, Zhen Ma and30. Shenghu Zhou.*Molecules*, 10(18): pp.12609-12620, 2013.
16. Bing-Xian Chung, Chuan-PuLiu . *Materials Letters*, 58: 1437–1440.
17. E.Sowka, M.Leonowicz, B.Andrzejewski A. D. Pomogailo G. I. Dzhardimalieva, *Materials Science poland*, 24(2),2006.
18. Ledo-Suárez,L.Rodríguez- Sánchez,M.C.Blanco,M.A.López-Quintela,phys.stat. sol,203(6):pp.1234 – 1240,2006. 32.
19. Mary donna BellelBalela , *Liquid-phase reduction and synthesis and characterization of cobalt nanoparticles prepared by liquid-phase reduction*, University Sains Malaysia, 2008. 33.
20. K.Rashmi, T.Krishnaveni, S.Ramanamurthy and P.Maruthi Mohan, *Characterization of cobalt nanoparticle from a cobalt resistant strain of neuro sporacra*, International Symposium of Research Students on Materials Science and Engineering December, Chennai, India, Department of Metallurgical and Materials Engineering, Indian Institute of Technology, Madras,2004.
21. R.Yogeswari, B.Sikha, Akshya Kumar, P.L. Nayak, *Journal of Microbiology and Antimicrobials*, 4(6):pp.103-109,2012.
22. M.A.Farooqui, P.S.Chauhan, P.Krishnamoorthy,J.Shai, *Journal of Nanomaterials and Biostructures*, 5:pp.43-49,2010.
23. DUAN Hongzhen, LIN Xiang yang, LIU Guanpeng, XU Lei and LI Fengsheng, *journal of Chem. Sci*,118(2):pp.179–184,2006.
24. R Venkat Narayan, Vinodkanniah and Aruna Dhathathreyan, *ChemSci Trans*, 2(1):pp.47-50, 2013.
25. Saeed Farhadi ,Jalil Safabakhsh and Parisa Zaringhadam ,*Journal of Nanostructure in a Chemistry*3(69),2013.
26. H. T. Yang, Y. K. Su,1, C. M. Shen, T. Z. Yang and H. J. Gao ,*Surface and Interface Analysis Surf. Interface Anal* 36:pp.155–160,2004.
27. C. Osorio-Cantillo A. N, Santiago-Miranda O, Perales-Perez and Y. Xin, *Journal of Applied Physics* 111,2012.
- Aher, R. H., Han, S. H., Vikhe, A. S., & Kuchekar, S. R. (2019). Green Synthesis of Copper Nanoparticles Using *Syzygium cumin* leaf extract, Characterization and Antimicrobial Activity. *Chemical Science Transaction*, 8(1), 1-6.
- He T, Chen D, Jiao X, Wang Y and Duan Y 2005 Solubility-controlled synthesis of high-quality Co₃O₄ nanocrystals *Chem. Mater.* **17** 15 4023-30
- Yulizar Y, Bakri R, Apriandanu D O B and Hidayat T 2018 ZnO/CuO nanocomposite prepared in one-pot green synthesis using seed bark extract of *Theobroma cacao* Nano-Structures & Nano-Objects **16** 300-5
31. Farhadi S, Javanmard M and Nadri G 2016 Characterization of cobalt oxide nanoparticles prepared by the thermal decomposition *Acta Chim. Slov.* **63** 2 335-43.
- Lu AH, Salabas EL & Schuth F (2007). Magnetic nanoparticles: synthesis, protection, functionalization, and application. *Angewandte Chemie International Edition* 46 (8): 1222–1244.
- Song Y, Modrow H & Henry LL (2006). Microfluidic synthesis of cobalt nanoparticles. *Chemistry of Materials* 18 (12): 2817–2827.

34. Pantes VF, Krishnan K & Alivisatos AP (2002).37. Synthesis of colloidal cobalt nanoparticles with controlled size and shapes. *Topics in Catalysis* 19 (2): 145–148.
35. Shah A, Haq S, Rehman W, Waseem M, Shoukat S and38. RehmanMU2019 *Mater. Res. Express* 6 1
36. Haq S, Dildar S, Ben Ali M, Mezni A, Hedfi A, ShahzadMI, ShahzadNand Shah A2021 *Mater. Res. Express* 8 055006
- Aisida SO, Ugwu K, Akpa P A, Nwanya AC, Ejikeme PM, Botha S, Ahmad I, MaazaMand Ezema F I 2019 *Mater. Chem. Phys.* 237 121859
- Zarei Z, RazmjoueDand Karimi J 2020 *Journal of Inorganic and Organometallic Polymers and Materials* 30 4606–14
39. ArsalanNet al 2020 *Int. J. Nanomed.* 15 4607
40. Khoshnamvand M, Ashtiani S, Huo C, Parsa S and Liu J 2019 *J. Mol. Struct.* 1179 749